The Effects of a Thin Liquid Layer on the Hydrodynamic Machine Rotor

Jaroslav Krutil, František Pochylý, Simona Fialová, Vladimír Habán

Abstract—A mathematical model of the additional effects of the liquid in the hydrodynamic gap is presented in the paper. An incompressible viscous fluid is considered. Based on computational modeling are determined the matrices of mass, stiffness and damping. The mathematical model is experimentally verified.

Keywords—Computational modeling, mathematical model, hydrodynamic gap, matrices of mass, stiffness and damping.

I. INTRODUCTION

IN all types of hydraulic machines are present hydrodynamic sealing gaps between the rotor and stator. Typical shape of the sealing gap is shown in Fig. 1.
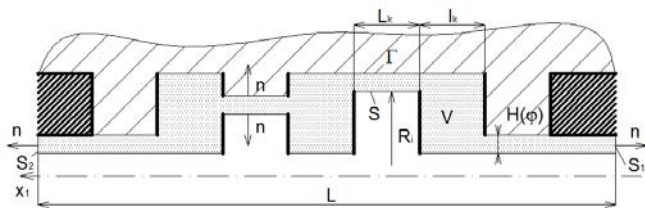

Fig. 1 Typical shape of the sealing gap

Fig. 2 shows the location of the hydrodynamic gaps in the interior of the centrifugal pump, or water turbines.
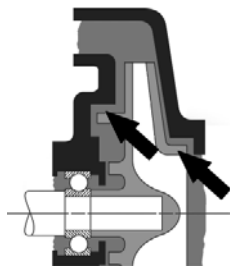

Fig. 2 Location of the hydrodynamic gaps in the interior of the centrifugal pump

It is assumed that the rotor has constant angular speed and performs the planar motion. Thus it does not move in the direction of the rotation axis. The fluid flows through the sealing gap due to the pressure gradient. While the rotor

J. Krutil is assistant in Power Engineering, Faculty of Mechanical Engineering, Brno University of Technology, Technická 2896/2; 616 69, Brno; CZ, (corresponding author; e-mail: jkrutil@seznam.cz).
F. Pochylý, professor, S. Fialová, assistant, and V. Habán, assistant, are with the Power Engineering, Faculty of Mechanical Engineering, Brno University of Technology, Technická 2896/2; 616 69, Brno; CZ, (e-mail: pochyly@fme.vutbr.cz, fialova@fme.vutbr.cz, haban@fme.vutbr.cz).

moves it leads to an interaction of the liquid with its surface. The i-th force component, which acts on the rotor as a result of this interaction, can be expressed as [1]:

$$F_i = \int_S \sigma_{ij} m_j dS \tag{1}$$

$$\sigma_{ij} = \eta \left(\frac{\partial v_i}{\partial x_j} + \frac{\partial v_j}{\partial x_i} \right) - p m_i. \tag{2}$$

The force **F** depends on the shaft translation **u**, velocity **u**˙ and acceleration **u**¨. In the case of the linear model it can be written [2], [3]:

$$\mathbf{F} = -(\mathbf{M}\mathbf{u}^{¨} + \mathbf{B}\mathbf{u}^{˙} + \mathbf{K}\mathbf{u}). \tag{3}$$

The solution goal will be determination of the matrix of additional mass **M**, additional damping **B** and additional stiffness **K**.

The mathematical model is valid only for small deflections from the equilibrium position (small eccentricity *e*). See Fig. 3.
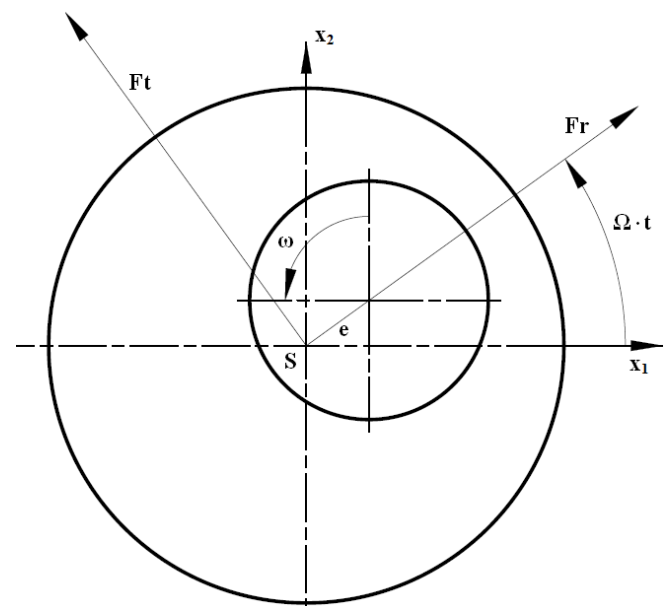

Fig. 3 The body motion in the incompressible liquid

In the case of large deviations from the equilibrium position are the matrices **K**, **B** dependent on **u** and **u**˙, according to:

$$\mathbf{B} = \mathbf{B}(\mathbf{u}, \mathbf{u}^{˙}); \mathbf{K} = \mathbf{K}(\mathbf{u}, \mathbf{u}^{˙}). \tag{4}$$

World Academy of Science, Engineering and Technology
International Journal of Mechanical and Mechatronics Engineering
Vol:9, No:6, 2015

In the paper it will be deal with the linear model (3), which is verified experimentally.

II. MATHEMATICAL MODEL

Assume that the shaft center performs a transient planar motion so that displacement vector **u** according to Fig. 3 is defined by:

$$\boldsymbol{u}^T(t) = \left(x_1(t)\,;\, x_1(t)\right) \tag{5}$$

The force acting on the rotor of the machine can be determined either in inertial space:

$$\boldsymbol{F}^T(t) = \left(F_{x1}(t)\,;\, F_{x1}(t)\right), \tag{6}$$

or no inertial space. See Fig. 3.

$$\boldsymbol{F}_r^T(t) = \left(F_r(t)\,;\, F_t(t)\right). \tag{7}$$

As previously stated, the goal is to identify matrices **M, B, K** and their verification. For this purpose, assume that the rotor carries excluding rotary and precession angular velocity Ω. See Fig. 3.

Under this assumption, can be written:

$$\boldsymbol{u}^T = e\boldsymbol{v}^T \;\; ; \;\; \boldsymbol{v}^T = (cos\Omega t, sin\Omega t). \tag{8}$$

The matrices **Γ, R, P** can be established by the terms:

$$\boldsymbol{\Gamma} = \left\| \begin{matrix} 0 & -1 \\ 1 & 0 \end{matrix} \right\| ; \boldsymbol{R} = \left\| \begin{matrix} cos\Omega t & -sin\Omega t \\ sin\Omega t & cos\Omega t \end{matrix} \right\| ; \boldsymbol{P} = \left\| \begin{matrix} F_r & -F_t \\ t_r & F_r \end{matrix} \right\| \tag{9}$$

Than it can be written:

$$\boldsymbol{F} = \boldsymbol{P}\boldsymbol{v} \;\; ; \;\; \boldsymbol{F}_r = \boldsymbol{R}^T\boldsymbol{F} \;\; ; \;\; \boldsymbol{F} = \boldsymbol{R}\boldsymbol{F}_r. \tag{10}$$

Considering (3), (8) can be written in the form:

$$\boldsymbol{F} = (-\boldsymbol{K} - \Omega\boldsymbol{B}\boldsymbol{\Gamma} + \Omega^2\boldsymbol{M})\boldsymbol{u}. \tag{11}$$

Substituting here from (10), it is obtained:

$$\boldsymbol{P} = (-\boldsymbol{K} - \Omega\boldsymbol{B}\boldsymbol{\Gamma} + \Omega^2\boldsymbol{M})e. \tag{12}$$

Hence the following relations come:

$$K_{11} = \boldsymbol{K}_{22} \;\; ; \;\; B_{11} = \boldsymbol{B}_{22} \;\; ; \;\; M_{11} = \boldsymbol{M}_{22}$$
$$K_{21} = -\boldsymbol{K}_{12} \;\; ; \;\; B_{21} = \boldsymbol{B}_{12} \;\; ; \;\; M_{21} = -\boldsymbol{M}_{12} \tag{13}$$

It is apparent that the matrices **M, B, K** are anti-symmetric, which may cause fatal consequences under certain conditions for rotor dynamics. For the force components F_r, F_t it can be written, assuming (13) based on (12):

$$F_r = -\left(K_{11} + \Omega B_{12} - \Omega^2 M_{11}\right)e \tag{14}$$

$$F_t = -\left(K_{21} + \Omega B_{22} - \Omega^2 M_{21}\right)e. \tag{15}$$

If F_r, F_t for different Ω can be specified, for example by computational modeling or experiment, it can be determined from (14) and (15), for example using the regression analysis, values of $K_{11}, B_{11}, M_{11}, K_{12}, B_{12}, M_{12}$.

III. COMPUTATIONAL MODELING

A mathematical model was verified based on the computational simulation and experiment. The shape of the hydrodynamic sealing gap is shown in Fig. 4 [4], [5].
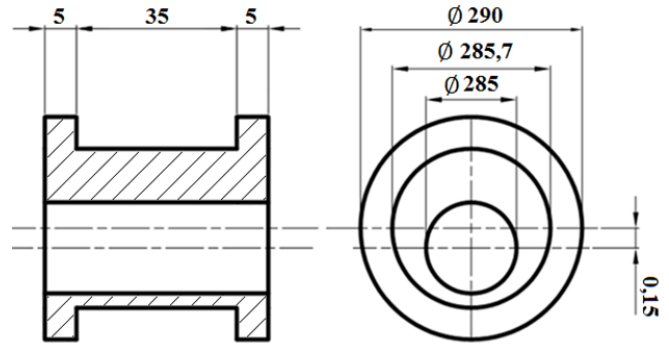

Fig. 4 The shape of the hydrodynamic sealing gap with the main dimensions (mm)

Fig. 4 shows the liquid layer. The rotor rotates at a constant angular speed ω = 314,1593 rad/s.

Precession rotor motion was calculated for the angular velocities: Ω_1 = 7,8539 rad/s; Ω_2 = 31,4159 rad/s; Ω_3 = 62,8319 rad/s; Ω_4 = 125,6637 rad/s; Ω_5 = 188,4956 rad/s; Ω_6 = 251,3274 rad/s; Ω_7 = 314,1593 rad/s.

Example of force calculations for the precession angular velocity Ω_3 = 62,8319 rad/s; is shown in Fig. 5 and for the precession angular velocity Ω_4 = 125,6637 rad/s; is show in Fig. 6.

Calculations were carried out in ANSYS FLUENT 15.0 for turbulence model standard $k - \varepsilon$ [6]. Dependence F_r and F_t were approximated by a polynomial of second order according to (14) and (15). From there were determined matrices of additional effects.

$$\mathbf{M} = \left\| \begin{matrix} 2,67 & 0 \\ 0 & 2,67 \end{matrix} \right\| [kg]; \tag{16}$$

$$\mathbf{B} = \left\| \begin{matrix} 1526 & -900 \\ 900 & 1526 \end{matrix} \right\| [kg/s]; \tag{17}$$

$$\mathbf{K} = \left\| \begin{matrix} 228 & 364240 \\ -364240 & 228 \end{matrix} \right\| \left[\frac{N}{m}\right]. \tag{18}$$

World Academy of Science, Engineering and Technology
International Journal of Mechanical and Mechatronics Engineering
Vol:9, No:6, 2015
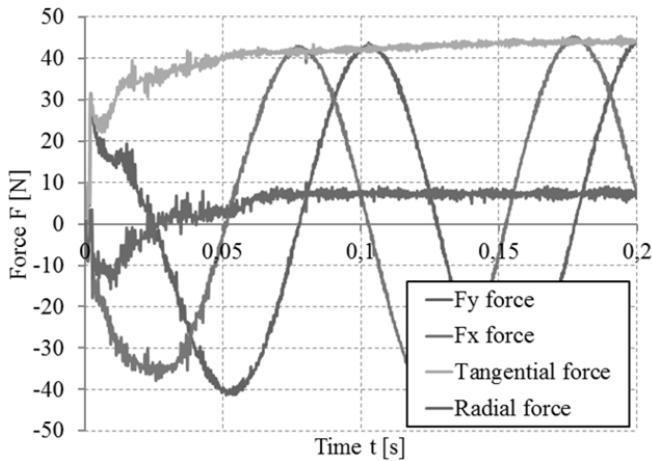

Fig. 5 Sample of progressions of forces for speed of precession
$\Omega_3 = 62,8319$ rad/s
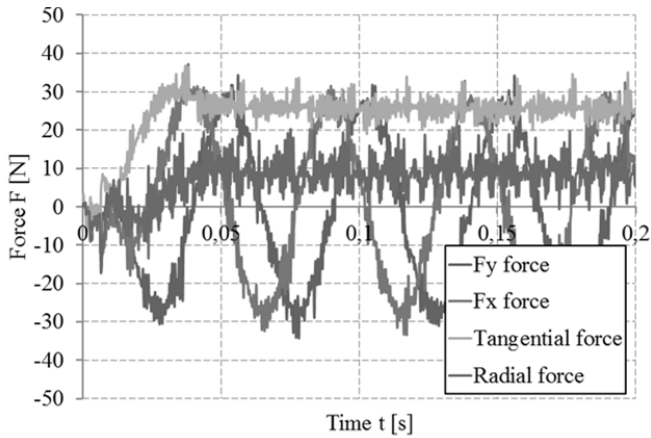

Fig. 6 Sample of progressions of forces for speed of precession
$\Omega_4 = 125,6637$ rad/s

IV. EXPERIMENT

The experiment was primarily focused at the stiffness matrix determination [7]. For this purpose was manufactured an experimental apparatus, whose principle is evident from Fig. 7. On Fig. 7 is shown the cut plane passing through the axis of rotation.
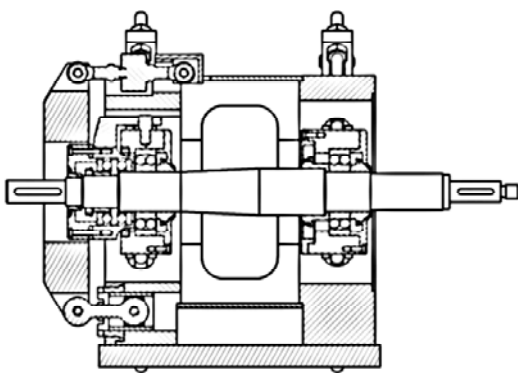

Fig. 7 Experimental Apparatus

The rotor is supported on roller bearings, which are placed on springs with strain gauge sensors. Both, the radial and tangential forces, are scanned.

The 3D model is shown in Fig. 8 where in the strain gauge sensors are obvious.
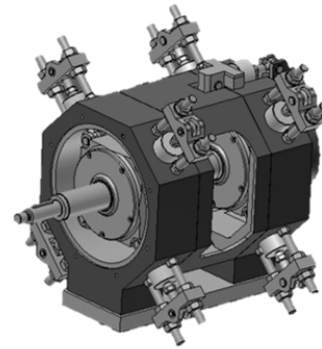

Fig. 8 3D model of experimental apparatus

On the shaft is mounted a disc, shown in Fig. 9 and formed a hydrodynamic gap. Before the disc is placed a bulky space where the water is supplied by the pipe (see Fig. 9). The overall layout of the actual design is shown in Fig. 10.
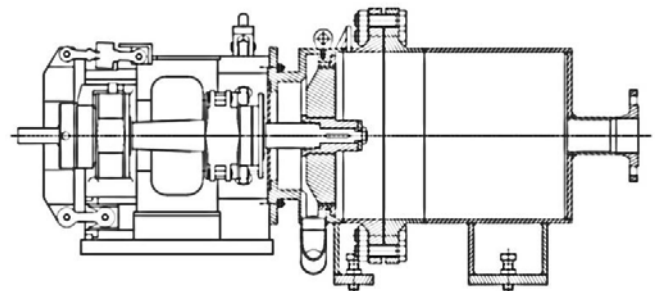

Fig. 9 Experimental apparatus with formed a hydrodynamic gap

The biggest problem in the experiment was correct setting of the shaft eccentricity and noise filtering. From the measured values of the forces in two orthogonal directions, the stiffness matrix was evaluated depending on the rotor speed.

For the measurements were used HBM strain gauge sensors (type U2, max. capacity 1000 kg, sensitivity 2mv / v).

World Academy of Science, Engineering and Technology
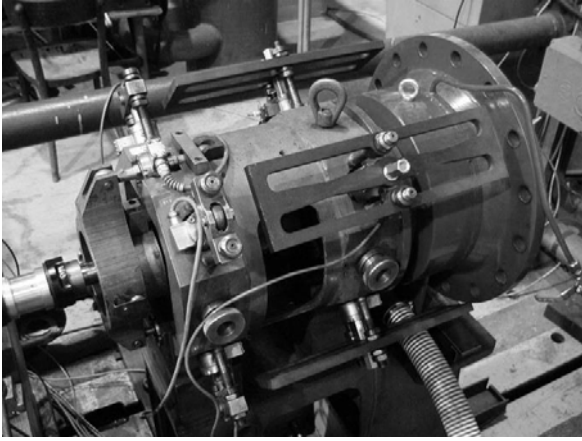International Journal of Mechanical and Mechatronics Engineering
Vol:9, No:6, 2015

Fig. 10 Photo of Experimental Apparatus

The results are shown in Fig. 11. From the measurement is obvious relatively large dispersion of the values that have been processed by statistical methods. In the graph are labeled points, which were compared with the computational simulation.

$$\mathbf{K}_{experiment} = \begin{Vmatrix} 0,25415 & 251,591 \\ -251,591 & 0,25415 \end{Vmatrix} [kN/m] \qquad (19)$$

$$\mathbf{K}_{numerical\ model} = \begin{Vmatrix} 0,228 & 364,24 \\ -364,24 & 0,228 \end{Vmatrix} [kN/m] \qquad (20)$$
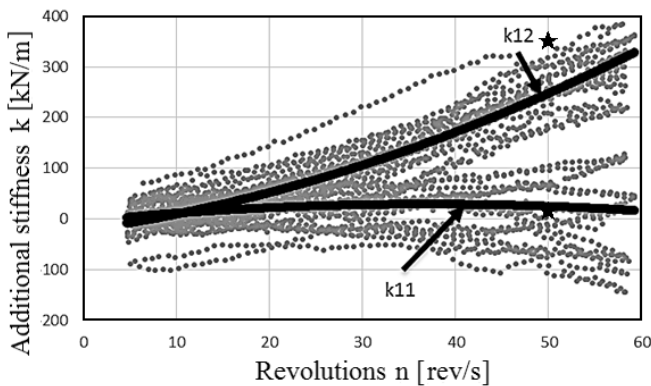

Fig. 11 The comparison of results from experiment (lines) and numerical model (stars)

ACKNOWLEDGMENT

REFERENCES

[1] A. Zagoruĺko, K. Gerasimiva, and E. Altuncev, "Čislennyj analiz ščelevych uplotněnnij", *12th International Scientific and Engineering conference (HERVICON 2008), Kielce-Przemysl, 9-12.September 2008. pp. 105-113, ISSN 1897-2683.*

[2] T. Staubi, and M. Bissing, "Numerically calculated rotor dynamic coefficients of a pump rotor side space", *Int. Symp. On Stability Control of Rotating Machinery (ISCORMA), South Lake Tahoe, August 2001.*

[3] C. Z. Kundera, A. Korczak, A. Zahorulko, K. Gerasimiva, and M. Plykin, "Numerical simulations of short and long annular seals", *Zeszyty Naukowy Politechniki Świetokrzyskiej, serija Budowa I Eksploatacja Maszyn, Kielce, 2007. No.7, C.77-8.*

[4] F. Pochylý, J. Krutil, "Hydrodynamic effects of the sealing gap", *Research Report number VUT-EU QR-33-13, Brno university of technology, 2013.*

[5] J. Krutil, F. Pochylý, S. Fialová, "Matrices of additional effects of the hydrophilic sealing gap of the hydrodynamic machine", *Riadenie tekutinových systémov XIV. International scientific and technical conference – Trečianske Teplice, SK, 2014. pp. 88-91, ISSN 978-80-970897-8-8*

[6] M. Athavale, and R. C. Hendricks, "A small perturbation CFD method for calculation of seal rotordynamics coefficients", *International Journal of Machinery, 1996, Vol. 2, No. 3., pp. 167-177.*

[7] Y. Kanemori, and T. Iwatsobo, "Experimental Study of Dynamics Fluid Forces and Moments for a Long Annular seals", *ASME Journal of Tribology, 1992, T.114, Oct., pp. 773-778.*